

# Determination of thermophysical properties of high temperature alloy IN713LC by thermal analysis

Simona Zlá<sup>1</sup>, Bedřich Smetana<sup>1</sup>, Monika Žaludová<sup>1</sup>, Jana Dobrovská<sup>1</sup>, Vlastimil Vodárek<sup>2</sup>, Kateřina Konečná<sup>2</sup>, Vlastimil Matějka<sup>3</sup>, Hana Francová<sup>1</sup>

<sup>1</sup>*VŠB-TU Ostrava, Faculty of Metallurgy and Materials Engineering, Department of Physical Chemistry and Theory of Technological Processes, 17. listopadu 2172/15, Ostrava-Poruba, Czech Republic*

<sup>2</sup>*VŠB-TU Ostrava, Faculty of Metallurgy and Materials Engineering, Department of Materials Engineering, 17. listopadu 2172/15, Ostrava-Poruba, Czech Republic*

<sup>3</sup>*VŠB-TU Ostrava, Nanotechnology Centre, 17. listopadu 2172/15, Ostrava-Poruba, Czech Republic*

00420 597 321 594

00420 597 323 396

[simona.zla@vsb.cz](mailto:simona.zla@vsb.cz)

**Abstract** The presented paper deals with study of thermophysical properties of cast, complex alloyed nickel based on superalloy Inconel 713LC (IN713LC). In this work the technique of Differential Thermal Analysis was selected for determination of the phase transformation temperatures and for the study of the effect of varying heating/cooling rate at these temperatures. The samples taken from as-received state of superalloy were analysed at heating and cooling rates of 1, 5, 10, 20 and 50 °C min<sup>-1</sup> with the help of the experimental system Setaram SETSYS 18<sub>TM</sub>. Moreover, the transformation temperatures at zero heating/cooling rate were calculated. The recommended values for IN713LC, after correcting to a zero heating rate, are 1205 °C ( $T_{\gamma',\text{solvus}}$ ), 1250 °C (solidus) and 1349 °C (liquidus). Influence of heating/cooling rate on shift of almost all temperatures of phase transformations was established from the DTA curves. Undercooling was observed at cooling process. The samples before and after DTA analysis were also subjected to the phase analysis with use of scanning electron microscopy on the microscope JEOL JSM-6490LV equipped with energy dispersive analyser EDAX (EDS INCA x-act). Documentation of the microstructure was made in the mode of secondary (SEI) and backscattered (BEI) electron imaging. On the basis of DTA analysis and phase analysis it may be stated that development of phase transformations of the alloy IN713LC will probably correspond to the following scheme: melting →  $\gamma$  phase; melting →  $\gamma$  + MC; melting → eutectics  $\gamma/\gamma'$ ; melting →  $\gamma$  + minority phases (e.g. borides); matrix  $\gamma \rightarrow \gamma'$ .

**Key words** DTA, IN713LC, temperatures of phase transformations, scanning electron microscopy

## Introduction

The aircraft industry often uses nickel superalloys for blades of the jet turbine engines. It is so because this material must satisfy numerous extreme requirements, such as e.g. heat resistance at high temperatures, resistance to fatigue damage, resistance to aggressive effect of flue gases, etc. [1, 2]. For these reasons it is necessary to pay attention to acquisition of reliable data, which are needed for modelling of processes, for control of solidification processes, but also for improvement of process procedures and for enhancement of their efficiency. Although material data (e.g. temperatures of phase transformations, latent heats) were measured also for some superalloys, so far no accessible database of thermophysical data of these systems exists [3-5].

Typical necessary data are temperatures of phase transformations [6-8], latent heats of phase transformations [9], specific heats [3] and other important data (thermal conductance, etc.). The obtained data should be used like input data for many simulation programs (simulation of the temperature and concentration fields in castings), numerical, physical models and requirements of practice (casting conditions) and they should contribute to explanation of mechanism of phase transformations of nickel based superalloys, which appear to be much more complex than it has been referred so far.

Differential Thermal Analysis (DTA) presents one possibility for describing thermal behaviour of nickel based superalloys and for verifying theoretical data. This method makes it possible to obtain thermophysical and thermodynamic data (such as temperatures of phase transformations, enthalpies of phase transformations, ...) not only of metallic systems.

This paper is devoted to cast superalloy IN713LC, which has been strengthened by precipitations (hardening phase  $\gamma'$ ), which are coherent with the matrix. Some already mentioned properties and ensuing wide use of these alloys result from this. Due to the fact that this alloy is used for production of components for gas turbines (stationary and aircraft turbines), which are exposed to extreme conditions, it is necessary to concentrate the attention on obtaining reliable thermophysical data. The obtained results should contribute to explanation of the mechanism of phase transformations occurring in the alloy IN713LC.

## DTA (Differential Thermal Analysis)

### Experiment

#### *Alloy Inconel 713LC (IN713LC)*

Cast, polycrystalline, nickel based superalloy IN713LC (Low Carbon) strengthened by precipitation was chosen as experimental material. It is a low-carbon modification of the alloy IN713C. It was developed for integrally cast rotor wheels and for independent rotor blades for gas turbines. Carbon content was reduced to prevent formation of carbides, which may to some limited extent act favourably on the grain boundaries against creep. However, type of carbides changes under effect of high-temperature and instead of small quantity of carbides of the MC type with high carbon content large quantities of low-carbon carbides of the type  $M_{23}C_6$  are created, which may form on the grain boundaries chains that consequently deteriorate creep properties. This means that higher content of carbon is in these alloys undesirable. For this reason boron was used for improvement of properties of grain boundaries. Due to very difficult machinability the components made of the alloy IN713LC were cast with only minimum allowances for machining. Typical technology for fabrication of castings is precise investment casting. Due to high content of elements reacting with oxygen it is necessary to apply vacuum technology. Casting temperature of the alloy IN713LC is usually 1389 °C for ensuring good fluidity, optimal mechanical properties and soundness of the casting. Control of casting temperature is crucial due to low content of carbon and its significant influence on the alloy properties [1, 10].

Material IN713LC was remelted in vacuum and cast by the company PBS Velká Bíteš, a.s. by investment casting into the mould. For the purposes of measurement of thermo-physical data of the alloy IN713LC the samples were not heat treated, they were used in as-received state. Chemical composition (wt.%) of the cast superalloy is given in Table 1.

#### *DTA, conditions of experiment*

Method of Differential Thermal Analysis (DTA) [11-13] was used for the purposes of measurement of temperatures of phase transformations. A rod with

diameter of approx. 3 mm was mechanically cut from the casting of the alloy and 5 samples with the height of approx. 3 mm and mass from 160 to 200 mg were cut from it.

Data were acquired with use of experimental laboratory equipment for thermal analysis SETSYS 18<sub>TM</sub> made by Setaram (Fig. 1). Samples of the alloy were analysed in corundum (Al<sub>2</sub>O<sub>3</sub>) crucibles with volume of 100  $\mu$ l. During heating/cooling a permanent dynamic atmosphere was maintained – flow rate of Ar (> 99.9999%) was 2 l h<sup>-1</sup>. The samples were during the experiment control heated at the rates of 1, 5, 10, 20 and 50 °C min<sup>-1</sup> within the temperature range from 20 to 1400 °C, the samples were after reaching the temperature of 1400 °C (after melting) control cooled by the above mentioned rates down to 20 °C.

## Results and discussion

It is possible to obtain the investigated temperatures of phase transformations from the so called DTA curves, which demonstrate heat phenomena during linear heating and cooling of samples. These curves are registered and evaluated on computer by the program SETSOFT. Figures 2 and 4 show for illustration DTA curves obtained at heating and cooling of the samples at the rate of 10 °C min<sup>-1</sup> with marking of characteristic temperatures of phase transformations.

Temperatures of phase transformations obtained during heating (Fig. 2, Table 2) were read from the DTA curves from the left to the right. The curves obtained at heating were characterised by two more distinct endothermic peaks. The first peak represents dissolution of the strengthening phase  $\gamma'$  and it is characterised by the temperature of the peak start ( $T_{\gamma',s}$  – initial temperature of dissolution of the phase  $\gamma'$ ) and by the temperature of the peak end ( $T_{\gamma',solvus}$  – final temperature of dissolution of the phase  $\gamma'$ ; temperature of solubility = „solvus“). Interval of temperatures corresponding to dissolution of the phase  $\gamma'$  comprises probably dissolution of particles of the phase  $\gamma'$  in the centre of dendrites and also in inter-dendritic spaces [12]. Kinetics of dissolution of these particles in the centre of dendrites and in inter-dendritic spaces will probably be different (centre of dendrites is enriched in Al, while inter-dendritic spaces are enriched in Ti). Due to the fact that dissolution of the phase  $\gamma'$  is very gradual and corresponding

thermal effects are small, it was impossible to separate these two thermal effects from the DTA curves, and to determine thus unequivocally the temperature of start and end of dissolution of this phase in dendrites and in inter-dendritic spaces. It is possible that in some superalloys a dissolution of other minority phases may occur in the area of dissolution of the phase  $\gamma'$  (such as phases  $\eta$ ; borides of the type  $M_3B_2$ ; ...) [13], which reflect the history of material preparation. In the case of the alloy IN713LC structural and phase analysis have found no particles of the above mentioned minority phases in the sample in initial state. For this reason the issues related to these minority phases are not discussed in this paper. The temperature interval between the temperatures  $T_{\gamma',\text{solvus}}$  and  $T_S$  (solidus temperature) is generally labelled as „heat treatment window”, Fig. 3. The second distinct peak reflects melting of the alloy, which comprises several processes (transformations), which follow closely one after another. These transformations run under temperature of full smelting of the alloy, i.e. below the liquidus temperature and they are characterised by small thermal effects.

It must be noted that in the modes of heating and cooling it is very difficult to read unequivocally the temperature of start of some peaks (temperatures of dissolution/precipitation of the phase  $\gamma' - T_{\gamma'}$ , temperatures of dissolution and formation of eutectics  $\gamma/\gamma'$ , temperatures of formation of carbides MC) – for this reason these temperatures are generally given in a temperature interval. Due to the need of assessment of the effect of varying heating/cooling rate on shifting of temperatures (extrapolation of temperatures to the zero heating/cooling rate) the temperatures were not summarised in the Tables 2 and 3 as temperature intervals, but as temperatures of starts (S = Start, e.g.  $T_{\gamma/\gamma',S}$ ), ends (E = End, e.g.  $T_{\gamma/\gamma',E}$ ). Due to the fact that intervals of temperature of solidus and dissolution (formation) of eutectics  $\gamma/\gamma'$  are identical, they are given in Tables 2 and 3 in one column, e.g.  $T_S$  ( $T_{\gamma/\gamma',S}$ ) or  $T_S$  ( $T_{\gamma/\gamma',E}$ ).

It seems that between the temperatures  $T_S$  and  $T_L$  a dissolution of the MC type carbides probably occurs. It is impossible to determine unequivocally the start of dissolution, because this is not an invariant reaction and dissolution occurs gradually in larger temperature interval. Due to the fact that structure of the alloy IN713LC may contain carbides of the type MC of various chemical composition, such as NbC, TiC, they are probably dissolved gradually. The carbides will be

dissolved at various temperatures within the interval of solidus and liquidus temperatures. It is possible that in the area between the temperatures  $T_S$  and  $T_L$  in some nickel superalloys a gradual dissolution may occur, or dissolution of some minority phases may continue (e.g. phase  $\eta$ ; borides of the  $M_3B_2$  type; inter-metallic particles Ni–Zr (probably  $Ni_7Zr_{12}$ )...) [13], which may reflect history of the material preparation. As it has already been stressed, in the case of the alloy IN713LC structural analyses did not find in the sample in initial state any particles of the above mentioned minority phases. In the same manner temperatures of phase transformations obtained at the heating rates of 1, 5, 20 and 50 °C min<sup>-1</sup> were evaluated from the measured DTA curves and they are summarised in Table 2.

The temperatures of phase transformations obtained during cooling (Fig. 4, Table 3) were read from the DTA curves from the left to the right. Start of the first distinct peak corresponds on the DTA curve to formation of the matrix  $\gamma$ , or to formation of dendrites of the phase  $\gamma$  (liquidus temperature –  $T_L$ ). Formation of the matrix is accompanied by segregation of elements with effective distribution coefficient  $k$  smaller than 1 into the remaining melt. In the case of the alloy IN713LC this is the case primarily of Nb ( $k = 0.04$ ), and Ti ( $k = 0.6$ ). Particles MC, namely NbC and TiC, are formed predominantly in inter-dendritic spaces as a result of oversaturation. Sharp rise of carbides volume is connected with distinct thermal effect. Start of carbides formation is marked as  $T_{MC,S}$ . Carbides are most probably formed by an eutectic reaction:  $L \rightarrow \gamma + MC$ , and one temperature should be attributed to their formation. However, it is evident from experimental measurements, that carbides are formed in a temperature interval, probably because of presence of carbides of various chemical composition. Kinetics of formation of these carbides will be different and it may be influenced by kinetics of formation of the matrix and of other minority phases that are present in structure of the alloy IN713LC.

During subsequent drop of temperature formations of non-equilibrium eutectics  $\gamma/\gamma'$  in the form of “crown” are formed in inter-dendritic spaces. These eutectics are most probably formed also by an eutectic reaction:  $L \rightarrow \gamma/\gamma'$ , but again in the temperature interval ( $T_{\gamma/\gamma',S}$  and  $T_{\gamma/\gamma',E}$ ). It followed from the experimentally obtained DTA curves, that solidification of alloy will most

probably end at the temperature  $T_S$ . It was found on the basis of structural analysis of the alloy IN713LC, that along part of the “crown” of eutectics coarse particles of the phase  $\gamma'$  were segregated. Elements with low solubility in the phases  $\gamma$  and  $\gamma'$  were probably during formation of eutectics pushed out into the last remainders of the melt, which might have caused drop of solidification temperature of these last islands of the melt. Solidification of enriched islands of the melt before the chain of coarse  $\gamma'$  particles in eutectics is in the literature [4, 14, 16] labelled as „terminal eutectic transformation“ and in the case of the alloys of the type IN713 the following minority phases may be formed as structural analysis has shown it: phase  $\eta$ , borides of the  $M_3B_2$  type, or inter-metallic particles Ni–Zr (probably  $Ni_7Zr_{12}$ ). Particles of the phase  $\eta$  were not found in the samples of investigated alloy IN713LC after controlled crystallisation, probably due to low content of Ti. Borides will be formed with the most probably in the area of temperatures  $T_{MC,E}$  and  $T_S$ . No specific temperature or marking was attributed to formation of borides and Ni–Zr particles, since they were represented in the samples after the controlled crystallisation only in minority quantity, and thermal effect corresponding to their formation is probably obscured by formation of carbides and non-equilibrium eutectics, which are characterised by higher thermal effect.

Below the temperature  $T_{\gamma',\text{solvus}}$  particles of the strengthening phase  $\gamma'$  will precipitate in solidified matrix during gradual cooling. Thermal effect related to precipitation of the phase  $\gamma'$  is comparatively small and very gradual. It is also very problematic to determine precisely the end of precipitation of the phase  $\gamma'$  ( $T_{\gamma',E}$ ). Kinetics of segregation of these particles of the phase  $\gamma'$  in the centre of dendrites and in inter-dendritic areas will be probably different (centre of dendrites is enriched in Al, while inter-dendritic areas are enriched in Ti). In the area of formation of the phase  $\gamma'$  the phase  $\eta$  may be formed, as well as inter-metallics Ni–Zr (probably  $Ni_7Zr_{12}$ ), or borides. As it has already been expressed, these phases may be formed at higher temperatures (between temperatures of liquidus and solidus), but at the same time they may be formed also in the area of precipitation of the phase  $\gamma'$ . Structural analysis revealed presence of inter-metallics, but only in minority quantity, that's why no specific value of temperature was attributed to this phase transformation. Borides were present only



in the sample that was control cooled at the rate of  $50\text{ }^{\circ}\text{C min}^{-1}$ , particles of the phase  $\eta$  were not present in the samples.

At evaluation of temperatures of phase transformations all the temperatures were corrected to the melting temperatures of standard metals (Au, Ni, purity 5N).

On the basis of experimentally obtained temperature the values of phase transformations temperatures at zero heating/cooling rate were obtained by extrapolation to the zero heating/cooling rate. It means that temperatures close to the equilibrium state were obtained, „0 (calc.)“. They are also given in Tables 2 and 3. For clearness and for better assessment of the effect of varying heating/cooling rate on shifting of transformation temperatures all the obtained DTA curves of the alloy IN713LC were brought for each thermal mode into one common image (Fig. 5a– heating; Fig. 5b – cooling).

Measurement of temperatures of phase transformations by various exactly defined rates, as well as extrapolation of these temperatures to the zero heating/cooling rate were performed in order to assess the influence of the mode rate on shift of temperatures of phase transformations. Heating or cooling rate influences formation/extinction of a certain phase, its existence, e.g. in which temperature interval it exists, which next phase will be formed and whether the transformation will run in a certain manner or by other mechanisms [3].

On the basis of experimental results and extrapolation an obvious influence of heating/cooling rate on shift of almost all temperatures of phase transformations was established from the DTA curves obtained during the controlled heating and cooling of the samples from the alloy IN713LC. In Fig. 5a and Table 2 shift of almost all temperatures of phase transformations was observed at the heating mode towards higher values with the increasing heating rate. From the perspective of technical practice one of the most important areas of temperatures of phase transformations of superalloys is the temperature interval between the temperatures  $T_{\gamma',\text{solvus}}$  and  $T_S$  (heat treatment window). Heating rate did not have any substantial influence on width of this interval. Width of the temperature interval was approx.  $40\text{ }^{\circ}\text{C}$ . Chapman [3] gives the width of this interval between 0 and  $71\text{ }^{\circ}\text{C}$ . Interval of melting (interval between  $T_S$  and  $T_L$ ) of the alloy was also not influenced significantly by the heating rate.



It is obvious from Table 3 and Fig. 5b, that cooling rate influences the shift of almost all measured transformation temperatures in such a manner, that temperature of the given transformation decreases with an increasing cooling rate. In case of cooling from the perspective of technical practice one of the most important areas of temperatures of phase transformations of superalloys is the area between the temperatures  $T_L$  and  $T_S$ . This interval of solidification obtained at the rates 1 to 20 °C min<sup>-1</sup> was almost identical. This interval was not influenced significantly in any way by the cooling rate.

The temperature interval corresponding to precipitation of the strengthening phase  $\gamma'$  (temperatures  $T_{\gamma',\text{solvus}}$  and  $T_{\gamma',E}$ ) is another important area. The broadest interval of precipitation of the phase  $\gamma'$  was observed in the sample that was control cooled at the rate of 50 °C min<sup>-1</sup>, where the interval was 258 °C. On the other hand, the narrowest temperature interval, namely 53 °C, was observed for the rate of 1 °C min<sup>-1</sup>. The temperature interval broadened with the increasing cooling rate. Identical trend was observed also in the temperature interval corresponding to dissolution of the phase  $\gamma'$  (heating of the samples of the alloy IN713LC).

Apart from investigation of influence of heating/cooling rate on the shift of temperatures of phase transformations, the influence of the mode of heating/cooling was also observed. DTA curves obtained during the controlled cooling realised at the rates given above, show and influence of undercooling on the samples of the alloy IN713LC, which might result in shifting of the temperatures of phase transformations obtained during the mode of cooling towards lower values, than the values of temperatures obtained at heating (Tables 2 and 3). Undercooling was observed in the whole area of temperatures of phase transformations. It is not possible on the basis of results of experimental measurements to observe unequivocally the temperature area with the highest or the lowest undercooling. It may be generally stated that undercooling was observed almost at all temperatures of phase transformations. Degree of undercooling of the nickel alloy IN713LC was influenced primarily by the heating/cooling rate. The biggest undercooling was observed always at the rate of 50 °C min<sup>-1</sup>, where it achieved even 62 °C. On the other hand the lowest undercooling occurred at extrapolated values of temperatures, or at the rate of 1 °C min<sup>-1</sup>. Almost at all temperatures of phase transformations an increase of the

degree of undercooling was observed with the increasing cooling rate. Values of some phase transformations of the alloy IN713LC obtained at cooling (DTA method) were found in available literature and they are also given in Table 3. It is evident from the obtained results that temperatures obtained experimentally in this work and temperatures published by the authors [17, 18] (Table 3) in some cases differ substantially. In spite of the fact that some authors investigate similar issues using similar experimental equipment, it is necessary to continue further investigation and research of the area of phase transformations of nickel based superalloys. Apart from the literature data, or calculated relations [19, 20] more and more perfect programs for calculation of thermo-physical and thermodynamic data exist nowadays [21, 22]. Nevertheless, no program exists, which would comprise all experimental and technological aspects that influence the resulting values (temperatures, heats of phase transformations). For these reasons it is necessary to create, disseminate and make more accurate the databases and programs as such – on the basis of new experimental and theoretical scientific findings.

## **Phase analysis of nickel based superalloy IN713LC**

### **Methodology of evaluation of structure**

The samples before and after DTA analysis were also subjected to the phase analysis with use of scanning electron microscopy on the microscope JEOL JSM-6490LV equipped with energy dispersive analyser EDAX (EDS INCA x-act). Documentation of the microstructure was made in the mode of secondary (SEI) and backscattered (BEI) electron imaging. The sample was chemically etched in solution of 100 ml H<sub>2</sub>O + 100 ml alcohol + 200 ml HCl + 5 g CuCl<sub>2</sub> in order to visualise its structure. Individual minority phases were identified on the basis of comparison of results of semi-quantitative EDX analysis with the published data on composition of phases occurring in the given type of nickel based superalloy. Semi-quantitative X-ray micro-analysis was performed only in the case of particles larger than 1 µm, when results were not significantly distorted by an X-ray signal from surrounding matrix. It may not be excluded that small particles of other minority phase might have been present in investigated samples.

## Analysis of the alloy by electron microscopy and micro-analysis

Micro-structure of the sample in as-received state and of all the samples after controlled crystallisation was qualitatively identical (Figs. 6 and 7): in metallic matrix  $\gamma$  particles of  $\gamma'$  phase were segregated, in inter-dendritic spaces the formations of eutectics  $\gamma/\gamma'$  were segregated. With the increasing cooling rate an increased occurrence of eutectic formations was observed. Share of these formations in molten and control cooled samples decreased with the decreasing cooling rate. Coarse particles of the phase  $\gamma'$  segregated along the part of perimeter of eutectic formations. In inter-dendritic spaces and similarly as along the grain boundaries, carbide particles MC segregated, where M represents namely Nb and Ti. Share of Mo and Zr in these particles was small. Shape and size of particles of the MC carbides in inter-dendritic spaces depended on conditions of cooling: the largest MC particles and at the same time their smallest frequency was determined in the sample, the cooling of which was the slowest ( $1\text{ }^{\circ}\text{C min}^{-1}$ ).

Particles of the following minority phases occurred in small quantities before the formations of eutectics  $\gamma/\gamma'$ : borides of the type  $\text{M}_3\text{B}_2$  [18]; compound carbides (particles MC rich in Zr nucleated on the surface of MC particles rich in Nb) [23]; inter-metallic particles Ni–Zr intergrown by the  $\gamma$  matrix – this is probably an eutectic [16, 24]. Occurrence of sulphides, or other minority phases was not found in the samples after DTA analysis. The phase  $\eta$  (hexagonal phase  $\text{Ni}_3\text{Ti}$ ) has also not been found in the samples – probably due to the low content of Ti in this alloy.

## Conclusions

In the presented work the temperatures of phase transformations at the precisely defined heating and cooling rates were experimentally investigated in real samples of nickel based superalloy IN713LC. On the basis of DTA analysis it is possible to draw following conclusions:

- Values of phase transformations temperatures at zero heating/cooling rate were obtained by extrapolation to the zero heating/cooling rate. It means that temperatures close to the equilibrium state were obtained, „0 (calc.)”, namely the

final temperature of dissolution of the phase  $\gamma'$  ( $T_{\gamma',\text{solvus}}$ , 1205 °C, heating), temperature of solidus (1250 °C, heating) and liquidus (1349 °C, heating), and other characteristic temperatures.

- Influence of heating/cooling rate on shift of almost all temperatures of phase transformations was established from the DTA curves obtained during the controlled heating and cooling of the alloy IN713LC. Heating rate did not have any substantial influence on width of the interval of heat treatment window. Width of the temperature interval was approx. 40 °C. Chapman [3] gives the width of this interval between 0 and 71 °C. Interval of melting of the alloy was also not influenced significantly by the heating rate. Interval of solidification obtained at the rates 1 to 20 °C min<sup>-1</sup> was almost identical. The temperature interval corresponding to precipitation of the strengthening phase  $\gamma'$  broadened with the increasing cooling rate (50 °C min<sup>-1</sup>, interval was 258 °C). Identical trend was observed also in the temperature interval corresponding to dissolution of the phase  $\gamma'$  (heating of the samples of the alloy IN713LC).

- DTA curves obtained during the controlled cooling show an influence of undercooling on the samples of the alloy IN713LC.

- It is evident from the obtained results that temperatures obtained experimentally in this work and temperatures published by the authors [17, 18] in some cases differ substantially. In spite of the fact that some authors investigate similar issues using similar experimental equipment, it is necessary to continue further investigation and research of the area of phase transformations of nickel based superalloys.

On the basis of DTA analysis and phase analysis it may be stated that development of phase transformations of the alloy IN713LC will probably correspond to the following scheme:

melting  $\rightarrow \gamma$  phase;

melting  $\rightarrow \gamma + \text{MC}$ ;

melting  $\rightarrow$  eutectics  $\gamma/\gamma'$ ;

melting  $\rightarrow \gamma +$  minority phases (e.g. borides);

matrix  $\gamma \rightarrow \gamma'$ .

**Acknowledgements** This study was supported by the project of the Ministry of Education, Youth and Sports of the Czech Republic No. MSM6198910013 and of the project of the Ministry of Industry and Trade No. FR-TI3/077.

## References

1. Durand – Charre M. The Microstructure of Superalloys. Amsterdam: OPA; 1997.
2. Davis JR. Nickel, Cobalt and Their Alloys. Ohio: ASM International; 2000.
3. Chapman LA. Application of High Temperature DSC Technique to Nickel Based Superalloys. J. Mater. Sci. 2004;39:7229-7236.
4. Zupanič F, Bončina T, Križman A, Tichelaar FD. Structure of Continuously Cast Ni-based Superalloy Inconel 713C. J. Alloy. Compd. 2001;329:290-297.
5. Antonsson T, Fredriksson H. The Effect of Cooling Rate on the Solidification of INCONEL 718. Metall. Mater. Trans. B-Proc. Metall. Mater. Proc. Sci. 2005;36B:85-96.
6. Smetana B, Zlá S, Dobrovská J, Kozelský P. Phase transformation temperatures of pure iron and low alloyed steels in the low temperature region using DTA. Int. J. Mater. Res. 2010;101:398-408.
7. Zlá S, Dobrovská J, Smetana B, Žaludová M, Vodárek V, Konečná K. Differential Thermal Analysis and Phase Analysis of Nickel Based Super-Alloy IN 738LC. METAL 2010: 19th International Metallurgical and Materials Conference. 2010;790-795.
8. Zlá S, Dobrovská J, Smetana B, Žaludová M, Vodárek V, Konečná K. Thermophysical and structural study of IN 792-5A nickel based superalloy. Metalurgija. 2012;51(1):83-86.
9. Smetana B, Žaludová M, Zlá S, Dobrovská J, Cagala M, Szurman I, Petlák D. Application of High Temperature DTA Technique to Fe Based Systems. METAL 2010: 19th International Metallurgical and Materials Conference. 2010:357-362.
10. Petrenec M, Obrtlík K, Polák J. High temperature low cycle fatigue of superalloys Inconel 713LC and Inconel 792-5A. KEM (Key Engineering Materials). 2007;348-349:101-104.
11. Gallagher PK. Handbook of Thermal Analysis and Calorimetry: Principles and Practice. 2nd ed. Elsevier; 2003.
12. Waclawska I, Szumera M. Use of thermal analysis in the study of soil Pb immobilization. J. Therm. Anal. Calorim. 2010;99:873-877.
13. Lazau I, Pacurariu C, Babut R. The use of thermal analysis in the study of Ca<sub>3</sub>Al<sub>2</sub>O<sub>6</sub> formation by the polymeric precursor method. J. Therm. Anal. Calorim. 2011;105:427-434.
14. Ojo OA, Richards NL, Chaturvedi MC. On incipient melting during high temperature heat treatment of cast Inconel 738 superalloy. J. Mater. Sci. 2004;39:7401-7404.
15. Seo SM, Kim IS, Lee JH, Jo CY, Miyahara H, Ogi K. Eta Phase and Boride Formation in Directionally Solidified Ni-Base Superalloy IN792 + Hf. Metall. Mater. Trans. A-Phys. Metall. Mater. Sci. 2007;38A:883-893.
16. Ojo OA, Richards NL, Chaturvedi MC. Study of the Fusion Zone and Heat-Affected Microstructures in Tungsten Inert Gas-Welded INCONEL 738LC Superalloy. Metall. Mater. Trans. A-Phys. Metall. Mater. Sci. 2006;37A:421-433.

17. Lekstrom M, D'Souza N, Dong HB, Ardakani MG, Shollock BA. Solidification Kinetics in the Ni-Base Superalloy IN713LC. TMS (The Minerals, Metals and Materials Society). 2007;29-33.
18. D'Souza N, Lekstrom M, Dai HJ, Shollock BA, Dong HB. Quantitative characterisation of last stage solidification in nickel base superalloy using enthalpy based method. Mater. Sci. Technol. 2007;23:1085-1092.
19. Mills KC, Youssef YM, Li Z. The Effect of Aluminium Content on Thermophysical Properties of Ni-based Superalloys. ISIJ International. 2006;46:50-57.
20. Mills KC, Youssef YM, Li Z, Su Y. Calculation of Thermophysical Properties of Ni-based Superalloys. ISIJ International. 2006;46:623-632.
21. MTDATA. <http://www.npl.co.uk/science-technology/advanced-materials/measurement-techniques/mtdata/> [cited 2011-10-20].
22. Thermo-Calc Software. <http://www.thermocalc.com/> [cited 2011-10-20].
23. D'Souza N, Dong HB, Ardakani MG, Shollock BA. Solidification Path in the Ni-base Superalloy, IN713 LC – Quantitative Correlation of Last Stage Solidification. Scr. Mater. 2005;53:729-733.
24. Ojo OA, Richards NL, Chaturvedi MC. Microstructural Study of Weld Fusion Zone of TIG Welded IN 738LC Nickel-based Superalloy. Scr. Mater. 2004;51:683-688.

## Figure captions

Fig. 1 Setaram SETSYS 18<sub>TM</sub> experimental equipment: 1 – balance beam; 2 – measurement bar; 3 – alumina tube; 4 – crucible with measured sample; 5 – crucible with comparative sample; 6 – temperature control thermocouple; 7 – graphite heating element; 8 – graphite felt sleeve, 9 – purge, primary vacuum; 10 – carrier gas (He > 99.9999%); 11 – furnace protective gas (Ar 99.999%); 12 – cooling water

Fig. 2 DTA curve of the alloy IN713LC (heating rate 10 °C min<sup>-1</sup>) with marking of characteristic temperatures;  $T_{\gamma',S}$  – initial temperature of dissolution of the phase  $\gamma'$ ;  $T_{\gamma',\text{solvus}}$  – final temperature of dissolution of the phase  $\gamma'$  (temperature of solubility = „solvus“);  $T_S(T_{\gamma/\gamma',S})$  – solidus temperature (initial temperature of dissolution of eutectics  $\gamma/\gamma'$ );  $T_{\gamma/\gamma',E}$  – final temperature of dissolution of eutectics  $\gamma/\gamma'$ ;  $T_{MC}$  – temperature of dissolution of MC type carbides;  $T_L$  – liquidus temperature

Fig. 3 Diagram of phase transformations running in nickel based superalloys (continuous lines mark temperatures of phase transformations, which can be read from the DTA curves more unequivocally; dashed lines symbolise temperatures, the evaluation of which on the basis of the DTA curves is very difficult) [3]

Fig. 4 DTA curve of the alloy IN713LC (cooling rate 10 °C min<sup>-1</sup>) with marking of characteristic temperatures;  $T_L$  – liquidus temperature;  $T_{MC,S}$  – initial temperature of formation of MC type carbides;  $T_{MC,E}$  – final temperature of formation of MC type carbides;  $T_{\gamma/\gamma',S}$  – initial temperature of formation of eutectics  $\gamma/\gamma'$ ;  $T_S(T_{\gamma/\gamma',E})$  – solidus temperature (final temperature of formation of

eutectics  $\gamma/\gamma'$ );  $T_{\gamma',\text{solvus}}$  – initial temperature of precipitation of the phase  $\gamma'$  (temperature of solubility = „solvus“);  $T_{\gamma',E}$  – final temperature of precipitation of the phase  $\gamma'$

Fig. 5 a) DTA curves of the alloy IN713LC (heating rates 1, 5, 10, 20 and 50 °C min<sup>-1</sup>); b) DTA curves of the alloy IN713LC (cooling rates 1, 5, 10, 20 and 50 °C min<sup>-1</sup>)

Fig. 6 a) SEI micrographs of IN713LC, cooling rate 20 °C min<sup>-1</sup>; b) BEI micrographs of IN713LC, cooling rate 20 °C min<sup>-1</sup>

Fig. 7 a) SEI micrographs of IN713LC, cooling rate 50 °C min<sup>-1</sup>; b) BEI micrographs of IN713LC, cooling rate 50 °C min<sup>-1</sup>



Fig. 1 Setaram SETSYS 18<sup>TM</sup> experimental equipment: 1 – balance beam; 2 – measurement bar; 3 – alumina tube; 4 – crucible with measured sample; 5 – crucible with comparative sample; 6 – temperature control thermocouple; 7 – graphite heating element; 8 – graphite felt sleeve, 9 – purge, primary vacuum; 10 – carrier gas (He > 99.9999%); 11 – furnace protective gas (Ar 99.999%); 12 – cooling water

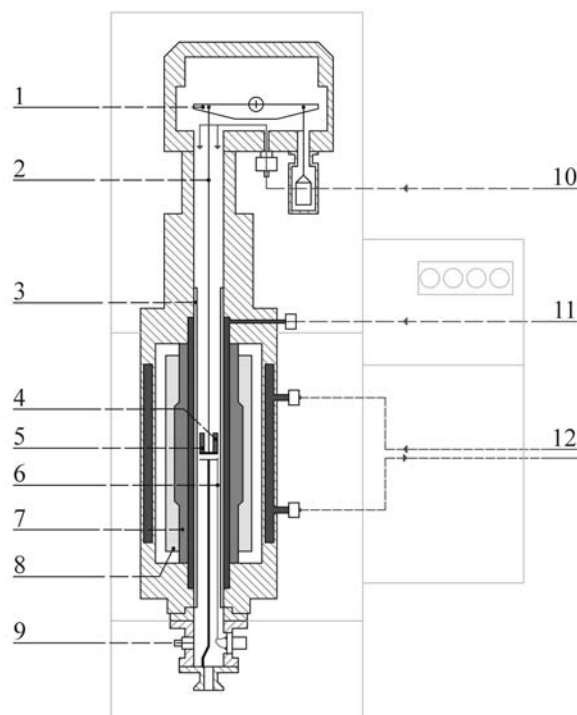


Fig. 2 DTA curve of the alloy IN713LC (heating rate 10 °C min<sup>-1</sup>) with marking of characteristic temperatures;  $T_{\gamma',S}$  – initial temperature of dissolution of the phase  $\gamma'$ ;  $T_{\gamma',\text{solvus}}$  – final temperature of dissolution of the phase  $\gamma'$  (temperature of solubility = „solvus“);  $T_S$  ( $T_{\gamma/\gamma',S}$ ) – solidus temperature (initial temperature of dissolution of eutectics  $\gamma/\gamma'$ );  $T_{\gamma/\gamma',E}$  – final temperature of dissolution of eutectics  $\gamma/\gamma'$ ;  $T_{MC}$  – temperature of dissolution of MC type carbides;  $T_L$  – liquidus temperature

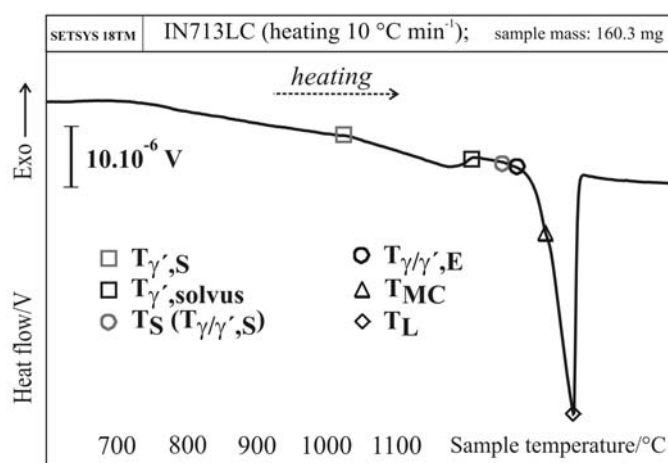


Fig. 3 Diagram of phase transformations running in nickel based superalloys (continuous lines mark temperatures of phase transformations, which can be read from the DTA curves more unequivocally; dashed lines symbolise temperatures, the evaluation of which on the basis of the DTA curves is very difficult) [3]

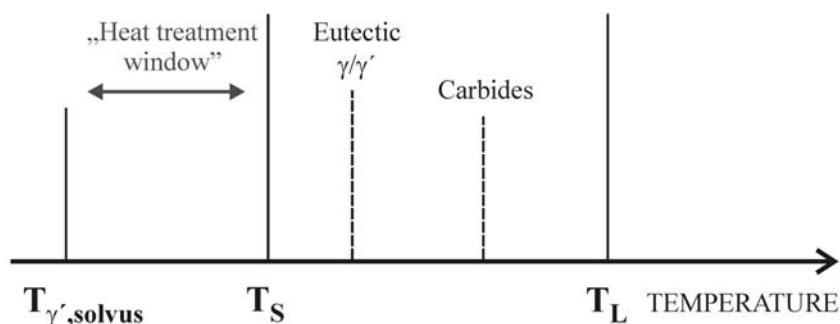


Fig. 4 DTA curve of the alloy IN713LC (cooling rate  $10\text{ }^{\circ}\text{C min}^{-1}$ ) with marking of characteristic temperatures;  $T_L$  – liquidus temperature;  $T_{MC,S}$  – initial temperature of formation of MC type carbides;  $T_{MC,E}$  – final temperature of formation of MC type carbides;  $T_{\gamma/\gamma',S}$  – initial temperature of formation of eutectics  $\gamma/\gamma'$ ;  $T_S$  ( $T_{\gamma/\gamma',E}$ ) – solidus temperature (final temperature of formation of eutectics  $\gamma/\gamma'$ );  $T_{\gamma',solvus}$  – initial temperature of precipitation of the phase  $\gamma'$  (temperature of solubility = „solvus“);  $T_{\gamma',E}$  – final temperature of precipitation of the phase  $\gamma'$

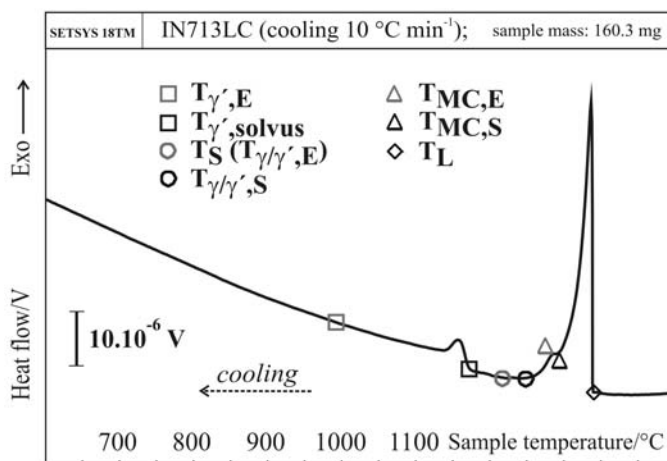


Fig. 5 a) DTA curves of the alloy IN713LC (heating rates 1, 5, 10, 20 and 50 °C min<sup>-1</sup>); b) DTA curves of the alloy IN713LC (cooling rates 1, 5, 10, 20 and 50 °C min<sup>-1</sup>)

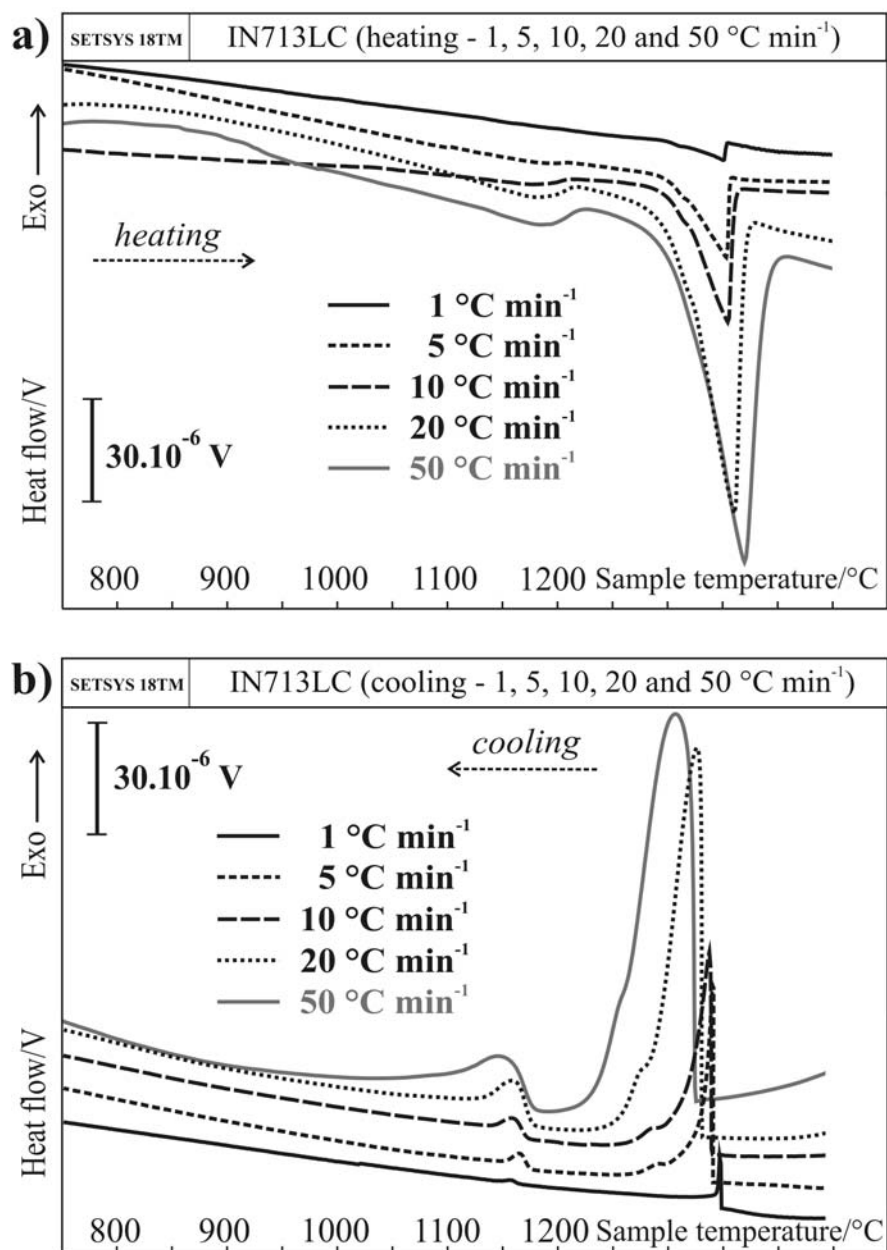


Fig. 6 a) SEI micrographs of IN713LC, cooling rate  $20\text{ }^{\circ}\text{C min}^{-1}$ ; b) BEI micrographs of IN713LC, cooling rate  $20\text{ }^{\circ}\text{C min}^{-1}$

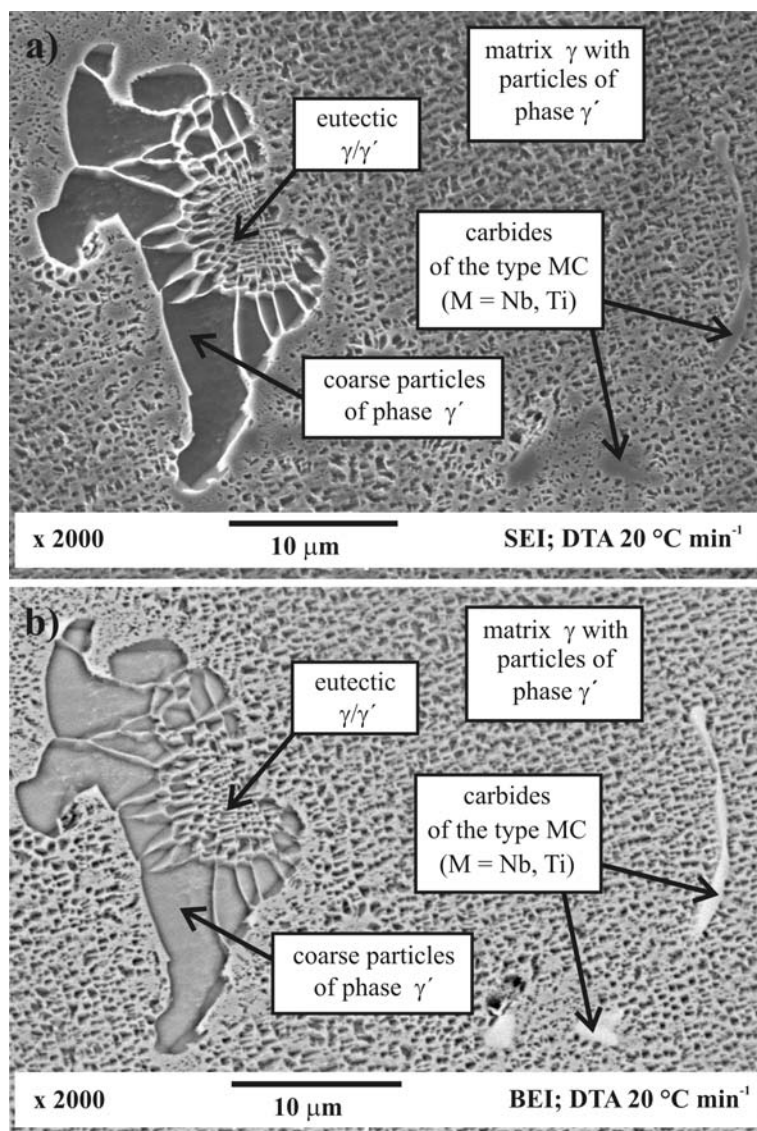


Fig. 7 a) SEI micrographs of IN713LC, cooling rate  $50\text{ }^{\circ}\text{C min}^{-1}$ ); b) BEI micrographs of IN713LC, cooling rate  $50\text{ }^{\circ}\text{C min}^{-1}$

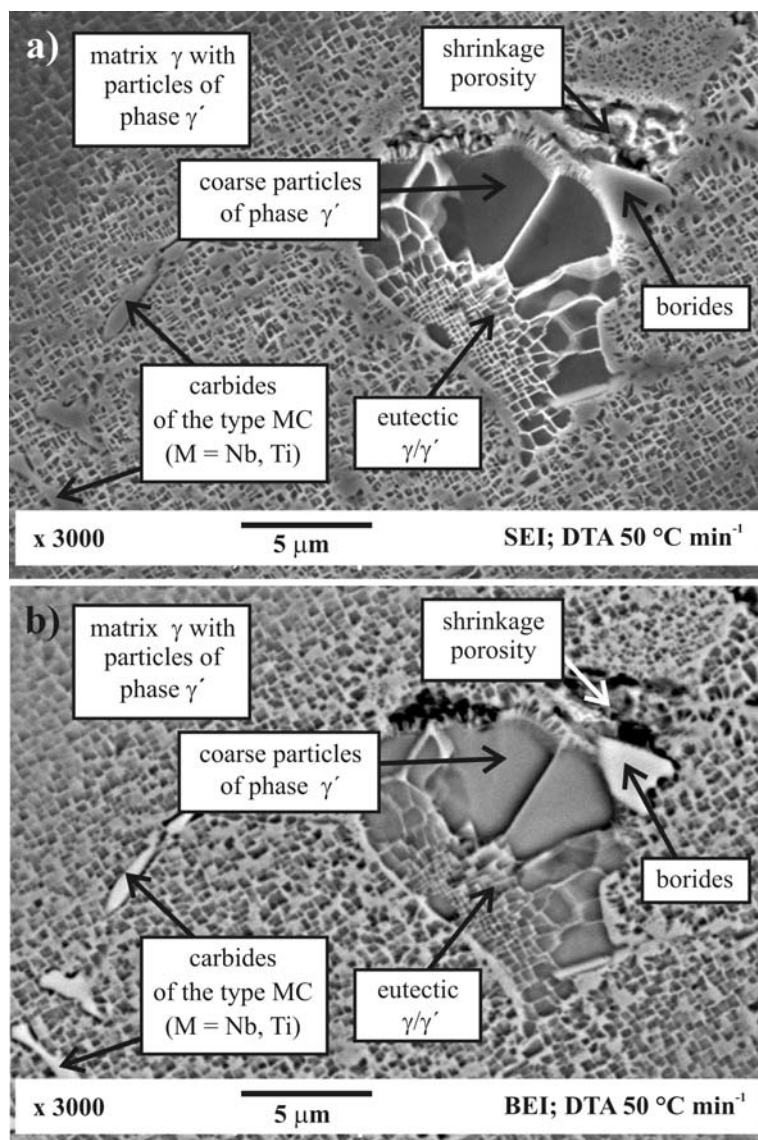


Table 1 Chemical composition of nickel based superalloy IN713LC/wt. %

Concentration of elements/wt. %								
Ni	Cr	Mo	Co	W	Al	Ti	Nb	Ta
base	12.00	4.68	0.41	-	5.90	0.77	2.31	< 0.05
Fe	C	Mn	Si	Cu	Zr	B	P	S
0.15	0.05	< 0.05	< 0.05	< 0.05	0.09	0.012	0.007	0.007

Table 2 Transformation temperatures of the alloy IN713LC for various heating rates

Heating rate /°C min <sup>-1</sup>	Temperature of phase transformation/°C					
	$T_{\gamma',S}$	$T_{\gamma',solvus}$	$T_S(T_{\gamma',S})$	$T_{\gamma',E}$	$T_{MC}$	$T_L$
50	987	1226	1252	1268	1325	1370
20	1003	1215	1253	1270	1322	1359
10	1029	1210	1253	1271	1319	1354
5	1101	1208	1248	1286	1318	1351
1	1133	1204	1248	1289	1316	1349
0 (calc.)	1094	1205	1250	1283	1317	1349

Table 3 Transformation temperatures of the alloy IN713LC for various cooling rates

Cooling rate /°C min <sup>-1</sup>	Temperature of phase transformation/°C						
	$T_L$	$T_{MC,S}$	$T_{MC,E}$	$T_{\gamma',S}$	$T_S(T_{\gamma',E})$	$T_{\gamma',solvus}$	$T_{\gamma',E}$
50	1324	1262	1249	1223	1193	1183	925
20	1329	1283	1270	1238	1213	1182	953
10	1338	1289	1286	1238	1219	1175	996
5	1339	1294	1290	1251	1227	1178	1084
1	1346	1341	1295	1262	1233	1167	1114
0 (calc.)	1343	1314	1294	1254	1230	1172	1074
5 [15]	1356	1312	1304	1278			
5 [16]	1355	1315		1281			